Charge Renormalization in Planar and Spherical Charged Lipidic Aqueous Interfaces

Federico Bordi,[†] Cesare Cametti,*[,†] Simona Sennato,[†] Beatrice Paoli,[†] and Carlotta Marianecci[‡]

Dipartimento di Fisica, Universitá di Roma La Sapienza, Piazzale A. Moro 5, I-00185 - Rome, Research Center SOFT-INFM-CNR, Unitá di Roma, and Dipartimento di Studi di Chimica e Tecnologia delle Sostanze Biologicamente Attive, Facoltá di Farmacia, Universitá di Roma La Sapienza, Rome, Italy

Received: October 12, 2005; In Final Form: January 12, 2006

The charge renormalization in planar and spherical charged lipidic aqueous interfaces has been investigated by means of thermodynamic and electrokinetic measurements. We analyzed the behavior of mixed DOTAP/DOPE monolayers at the air−electrolyte solution interface and DOTAP/DOPE liposomes 100 nm in size dispersed in an aqueous phase of varying ionic strength. For the two systems, we have compared the "effective" surface charge derived from the measurements of surface potential and ζ-potential to the "bare" charge based on the stoichiometry of the lipid mixture investigated. The results confirm that a strong charge renormalization occurs, whose strength depends on the geometry of the mesoscopic system. The dependence of the "effective" charge on the "bare" charge is discussed in light of an analytical approximation based on the Poisson−Boltzmann equation recently proposed.

1. Introduction

Complexes formed by polyelectrolytes and oppositely charged mesoscopic vesicles exhibit a rich and interesting phenomenology showing different self-assembled structures which find applications in different fields of advanced technologies, such as, for example, in templates for nanostructure construction[1] or in drug delivery.[2,3]

Because of the experimentally accessible length and time scales that make colloids a useful and intriguing model system for soft-matter physics, aggregation processes both in equilibrium and in nonequilibrium conditions have been extensively investigated. Recently, there has been renewed interest in colloidal systems with short-range attraction and long-range screened electrostatic repulsion.[4−7] However, a quantitative description of the effective interactions between charged particles, at a mesoscopic-scale level, is still an open question.[8]

Since electrostatic interactions are mainly responsible for the overall behavior of these mesoscopic systems, controlling a variety of effects such as colloidal stability and structural ordering,[9] the so-called effective particle electrical surface charge is a relevant parameter that plays a central role in the complex phenomenology these systems present.

A variety of experimental and theoretical investigations[8,10−14] suggests that the effective charge Q_{eff} of particles of mesoscopic size in colloidal suspensions is considerably smaller than the "structural" surface charge estimated, for example, by titration, indicating that, in different experimental conditions, the bare charge Q_{bare} should be replaced by a renormalized one. Moreover, nonlinear contributions cause the effective surface charge to be considerably smaller (for more than 1 or 2 orders of magnitude[11−14]) than the fully dissociated surface charge.

This effect is generally accounted for by considering that most of the charges, deriving from the ionization of the surface charged groups or from the dissociation of added simple salts, remain electrostatically bound to the particle or remain in its immediate vicinity.

Consequently, the concept of counterion condensation was coming out, and although proposed originally by Oosawa[15] and later by Manning for linear polyelectrolytes,[16,17] it has also been extensively employed in the case of spherical particle colloids.[18,19] A detailed analysis of these effects and an interesting discussion on the possible difference between charge renormalization and counterion condensation has been put forward by Quesada-Perez et al. in their recent review.[8]

These effects are generally described theoretically by the presence of an inner compact layer of strongly adsorbed counterions and a diffuse layer of relatively free ions to which the Debye−Hückel description applies with an effective charge.[10,12−14] Recently, direct measurements using optical tweezers on isolated pairs of charged spheres provided new experimental evidence for the exponential form of the far-field pair potential.[11,20] However, the structure and dynamics of the double layer are difficult to investigate experimentally, because of the small length scales and the short time scales involved, and only under special circumstances can direct information on the counterion distribution close to a charged surface be obtained.

From an experimental point of view, structural parameters such as the ion concentration and the stoichiometric surface charge are generally known, but their effective values are usually estimated from the data using a suitable model, and often different experimental approaches give rise to different estimates for the same parameter.[12] Although in some cases the estimates of their effective values are completely satisfactory, a more detailed understanding of the structure of charge interfaces would be desirable, particularly in the case of biological systems, where local pH and adsorption of small ions can potentially have strong effects on their conformation and functionality.[21−23]

In this work, we have investigated the electrical properties of two different lipidic aqueous interfaces with different curvatures, realized by a planar lipid monolayer at the air−

* To whom correspondence should be addressed. E-mail: cesare.cametti@roma1.infn.it. Fax: +39 06 4463158.

[†] Dipartimento di Fisica, Universitá di Roma La Sapienza, and Research Center SOFT-INFM-CNR.

[‡] Facoltá di Farmacia, Universitá di Roma La Sapienza.

10.1021/jp055821a CCC: $33.50
Published on Web 02/15/2006

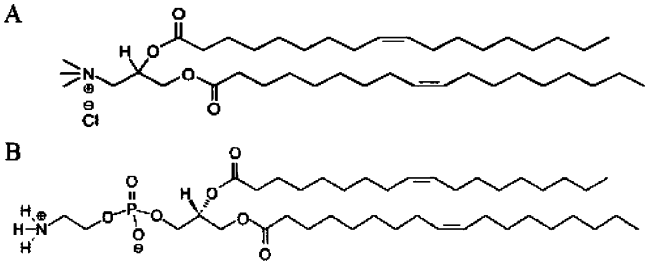

Figure 1. Chemical structure of the two lipids employed: (A) DOTAP. (B) DOPE.

water interface and by a closed spherical bilayer in a bulk aqueous suspension, respectively. The "stoichiometric" surface charge density of the two interfaces has been varied by employing a mixture of cationic (DOTAP) and neutral (DOPE) lipids in a controlled composition. Preliminary measurements of the surface isotherms (surface pressure vs area per molecule) ensure the almost ideal miscibility of the two lipids. The influence of the ionic strength of the subphase, in the case of the monolayers, and of the external suspending medium, in the case of the lipid vesicles, has been investigated by varying the content of a simple electrolyte (NaCl).

The effective surface charge, influencing the behavior of the system as viewed from the bulk external medium, has been evaluated from the measurement of two electrochemical parameters, i.e., the surface potential Ψ_0, in the case of a planar surface at the lipid−water interface, and the electrokinetic ζ-potential of the lipid vesicles, in the case of a spherical surface. This effective charge has been compared with the structural charge derived from the full ionization of the surface charged groups at the two interfaces.

Our results show that, in both cases investigated, a strong charge renormalization must be invoked to account for the measured values. The strength of this effect is different in the two experimental conditions. Moreover, our findings offer some further experimental evidence for the functional dependence of the effective charge Q_{eff} on the bare charge Q_{bare}, in light of an analytical approximation based on the Poisson−Boltzmann mean-field theory.

2. Experimental Section

2.1. Materials. *N*-[1-(2,3-dioleoyloxy)propyl]-*N*,*N*,*N*-trimethylammonium chloride [DOTAP] and 1,2-dioleoyl-*sn*-glycero-3-phosphatidylethanolamine [DOPE], specified as 99% pure, were purchased by Avanti Polar Lipids, Inc., and used without further purification. The chemical structures of the two lipids employed are shown in Figure 1.

Pure and mixed lipids were dissolved in chloroform or chloroform−methanol (1:1 v/v) to a final concentration of 1.6 mg/mL. In surface pressure measurements, the subphase was 0.1 M NaCl (Merck), while in surface potential measurements, the subphase was prepared using different concentrations of NaCl (between 1 mM and 1 M). All the electrolyte solutions were prepared using Milli-Q grade deionized water (Millipore), with an electrical conductivity less than 1 μS/cm.

2.2. Cationic Liposome Preparation. DOTAP and DOTAP/DOPE mixed liposomes were prepared by the lipid film hydration method. Lipid mixtures were dissolved in methanol−chloroform (1:1 v/v), and after a 3 h vacuum evaporation of the organic solvents, the resulting lipid film was rehydrated with Milli-Q quality water. The rehydration process was carried out for 1 h at a temperature of 42 °C, well above the main phase transition temperature of this lipid ($T_M \approx 0$ °C for DOTAP). To form small unilamellar vesicles, the lipid solution was sonicated at a temperature of 25 °C, for 1 h in the case of DOTAP/DOPE mixtures, at a pulsed power mode and extruded through Millipore 0.45 μm polycarbonate filter. The final liposome concentration was 1.6 mg/mL, and the solution was stored at 4 °C. Liposome size and size distribution were checked by standard dynamic light scattering measurements.

2.3. ζ-Potential Measurements. The ζ-potential measurements were carried out by means of the laser Doppler electrophoresis technique using a MALVER Zetamaster apparatus equipped with a 5 mW He−Ne laser. The mobility u was converted into the ζ-potential using the Smoluchowski relation $\zeta = u\eta/\epsilon$, where η and ϵ are the viscosity and the permittivity of the solvent phase, respectively.

2.4. Monolayer Surface Pressure Measurements. Mixed DOTAP/DOPE monolayers at different molar fractions were prepared at the air−water interface according to the Langmuir technique.[24] Surface tension measurements were carried out by means of the Wilhelmy plate technique with the trough (Minitrough, KSV, Finland) enclosed in a Plexiglas box to reduce surface contamination. Appropriate amounts of the lipid solution were spread by a microsyringe onto the aqueous subphase; after the deposition, the solvent was allowed to evaporate for 5 min before beginning the compression. Symmetric compression was performed with two moving barriers at a constant rate of 30 mm min^{-1}. Before each measurement, the trough was washed with chloroform and rinsed thoroughly with deionized water.

All measurements have been performed at the temperature of 25.0 ± 0.2 °C; the reproducibility of the surface pressure, at the same area per molecule, was within ±1 mN/m. Results reported here represent average values on three different isotherms, at least. The isotherms showed satisfactory reproducibility.

2.5. Monolayer Surface Potential Measurements. Surface potential measurements were performed using the noncontact, vibrating plate capacitor method, originally introduced by Lord Kelvin and improved by Yamins and Zisman.[25,26] We used a computer-controlled device (SPOT1, KSV), with a 17-mm-diameter active electrode, placed at few millimeters above the air−water interface, and a stainless steel reference electrode immersed in the subphase.

The surface pressure and surface potential were measured simultaneously during the film compression. At the beginning of each experiment, the surface potential of the aqueous phase was measured, and this value was assumed as reference. Before compression, a sufficiently long waiting time was required to allow the complete evaporation of the solvent for a good stabilization of the initial value of the surface potential.

We adjusted the probe parameter settings in order to reduce the capacitance effect due to the small variation of the electrode distance from the interface to a negligible extent, in different measurements. The reproducibility of the surface potential ΔV was within ±10 mV.

3. Results and Discussion

3.1. Planar Interfaces. Some typical results of the surface pressure and surface potential versus area isotherms of pure DOTAP and DOPE lipid monolayers and mixed DOTAP/DOPE lipid monolayers at the air−water interface are shown in Figure 2.

Pure DOTAP and DOPE monolayers exhibit, at the same temperature, isotherms characteristic of a single phase (a homogeneous liquid expanded fluid phase). The isotherms for

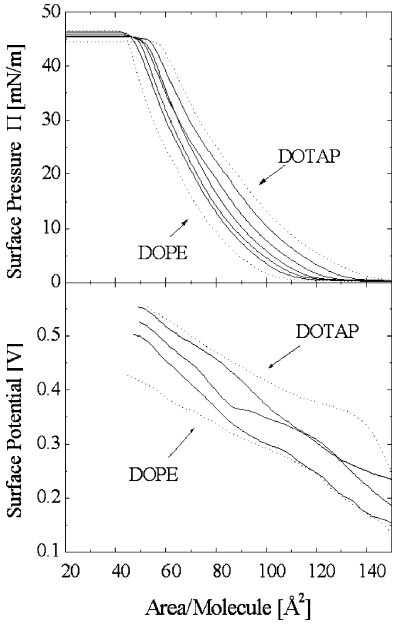

Figure 2. Surface pressure Π (upper panel) and surface potential (lower panel) vs area per molecule isotherms for DOTAP and DOPE pure monolayers and DOTAP−DOPE mixed monolayers. The curves falling between those of the pure lipid monolayers refer to some selected different DOTAP−DOPE composition. In the upper panel, from DOTAP to DOPE curves, the molar fractions of DOTAP are 0.8, 0.65, 0.5, 0.35, and 0.15, respectively. In the lower panel, for clarity of presentation, only the curves at mixed DOTAP 0.8, 0.5, and 0.35 molar fraction are presented. The subphase is 0.1 M NaCl; the temperature is fixed to the value of 25 °C within 0.2 °C.

the mixed DOTAP/DOPE films fall between those of the pure lipid monolayers. Starting from the pure DOTAP film, the progressive decrease of the DOTAP molar fraction, from 1 (pure DOTAP film) to 0 (pure DOPE film), results in a gradual shift of the isotherm toward smaller molecular areas, without affecting the overall curve shape, because of the decrease of the electrostatic repulsion between DOTAP polar heads.

The behavior of DOTAP/DOPE mixed monolayers can be studied by a surface thermodynamic analysis. The area per molecule in an ideal mixed two-component monolayer can be calculated from the relationship

$$A_{id} = X_1A_1 + X_2A_2 \tag{1}$$

where A_1 and A_2 are the areas per molecule of the pure components at the same surface pressure and X_1 and $X_2 = (1 - X_1)$ their mole fractions. The interactions between the two components, at a constant surface pressure and temperature, can be evaluated from the excess Gibbs free energy of mixing ΔG by integration of the surface pressure−area ($\Pi - A$) isotherm of mixed monolayers, from zero to different values of the surface pressure, according to the expression

$$\Delta G = \int_0^{\Pi} (A_{12} - X_1A_1 - X_2A_2)\, d\Pi \tag{2}$$

where A_{12} is the average area per molecule of the mixed monolayer.

In the absence of any specific interaction between the two components, $\Delta G = 0$. Deviations from an ideal behavior result in $\Delta G < 0$ (attractive interactions) or in $\Delta G > 0$ (repulsive interactions), providing information on whether a particular interaction is energetically favored or not in comparison to an ideal mixture, where the assumption of no intermolecular interactions is taken.

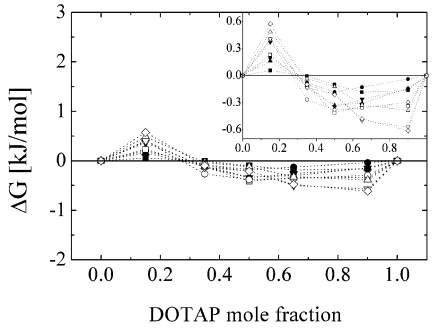

Figure 3. The excess free energy of mixing ΔG of mixed DOTAP−DOPE monolayers as a function of DOTAP composition, calculated at different surface pressures: (■) 5 mN/m; (●) 10 mN/m; (▲) 15 mN/m; (▼) 20 mN/m; (□) 25 mN/m; (○) 30 mN/m; (△) 35 mN/m; (▽) 40 mN/m; (◇) 45 mN/m. The horizontal dashed line is drawn to guide the eye only. Errors on ΔG derived from the surface molecular area integration have been quoted to be within some percent. The inset shows the small dependence on the monolayer composition in a magnified scale.

The excess free energy ΔG for DOTAP/DOPE mixtures at the different molar ratios investigated, from 5 to 40 mN/m, is shown in Figure 3.

In the case of mixed DOTAP/DOPE monolayers, the excess free energy ΔG is approximately zero for each mixture investigated. This means that DOTAP/DOPE mixtures behave, from a thermodynamic point of view, like an ideal mixture, that is, DOTAP and DOPE molecules behave as if they were of the same type.

During the compression of the film, for each mixed DOTAP/DOPE monolayer, the surface potential was also measured. The quantity ΔV represents the difference between the electric surface potential values measured in the monolayer-covered and monolayer-free (before spreading) subphases, which is taken as reference. The results are shown in Figure 2 (lower panel).

Surface potential results from the superposition of different contributions ranging from the dipole moments of the molecules forming the film to the change in orientation of the water molecules at the film−subphase interface. Moreover, in the case of charged monolayers (DOTAP is an ionic lipid), other contributions arise from the ionic double layer because of the presence of a diffuse-space charge from the counterions released into the aqueous subphase.[27,28] The overall surface potential can be related to the dipole moment of the molecules forming the film through the Helmholtz equation[27]

$$\Delta V = \frac{\mu_N}{A\epsilon_0\epsilon_r} + \psi_{GC} \tag{3}$$

where ϵ_r and ϵ_0 are the effective permittivity values within the layer and the dielectric constant of free space, respectively, μ_N is the normal component of the dipole moment per molecule, A the area occupied by each molecule, and ψ_{GC} the diffuse double layer contribution (the so-called Gouy−Chapman double layer), relative to the aqueous phase containing counterions.

The double layer contribution ψ_{GC} in eq 3 arises from the presence, in the subphase, of a diffuse-space charge due to the counterions, i.e., ions resulting from the ionization of ionic lipids and the ions resulting from the dissociation of the simple salt (NaCl) dissolved into the subphase. In our case, the ionic lipid is the DOTAP molecule that, by releasing Cl^- ions, imparts a positive charge to the film that can be evaluated as a function of the molar fraction of this component. The potential ψ_{GC} can be obtained by solving the Poisson−Boltzmann equation within the so-called Gouy−Chapman model.[29]

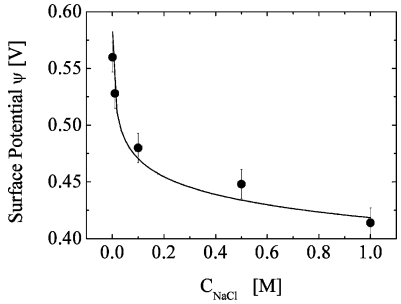

Figure 4. A typical dependence of the surface potential as a function of the salt concentration in the subphase. The values reported refer to DOTAP monolayer at molecular area of 70 Å^2. The full line is the calculated value on the basis of eqs 3 and 5.

Figure 2 (bottom panel) shows the surface potential ΔV as a function of the area A per molecule. The shape of these curves for mixed DOTAP/DOPE films changes smoothly from pure DOTAP to pure DOPE, as is to be expected when intermolecular interactions do not affect the orientation of the dipole moment and/or the effective permittivity of the layer.

To evaluate the effects induced by the ionic Gouy−Chapman double layer in the presence of charged interfaces, we performed surface potential measurements with subphases at various NaCl salt concentrations (between 1 mM and 1 M). Surface potential curves were analyzed by means of the Grahame equation

$$\sigma = \pm\sqrt{2RT\epsilon\sum_i c_i^0[\exp(-z_i F\psi_{GC}/RT)] - 1} \qquad (4)$$

where σ is the surface charge density at the monolayer interface and c_i^0 is the ionic species concentration in the bulk phase. In the case of two ionic species (Na^+ and Cl^- ions due to the sodium chloride ionization), neglecting counterions deriving from the ionization of DOTAP polar heads, eq 4 can be rearranged as

$$\psi_{GC} = \frac{K_B T}{ze}\cosh^{-1}\left(1 + \frac{\pi l_B}{A_c^2 C_{NaCl}}\right) \qquad (5)$$

where A_c is the effective area per charge at the monolayer interface and l_B the Bjerrum length ($l_B = (e)^2/4\pi\epsilon_0\epsilon K_B T$).

The total measured potential ΔV is due to the sum of the dipole moment $\psi_0 = (\mu_N/A\epsilon_0\epsilon_r)$ of molecules forming the film and, in the case of charged monolayers, of the Gouy−Chapman potential ψ_{GC}.

A typical dependence of ΔV as a function of the salt concentration in the case of a DOTAP monolayer at a molecular area of 70 Å^2 is shown in Figure 4.

The parameters ψ_0 and A_c for each DOTAP/DOPE monolayer investigated were derived by a nonlinear least-squares fitting procedure of eqs 3 and 5 to the measured values of the surface potential ψ obtained, at the same area per molecule, for different values of the salt concentration in the subphase.

The results of this analysis are shown in Figure 5, where the behavior of the quantities ψ_0 and A_c are reported as a function of DOTAP molar fraction, at some selected values of the area per molecule (different monolayer surface pressures).

The contribution ψ_0 of the surface potential due to the dipole moment of the lipid headgroups is approximately independent of the monolayer composition but increases with the decrease of the monolayer surface pressure. This behavior can be justified by considering that, with the increase of the surface pressure, molecules are forced to rearrange themselves into a smaller area,

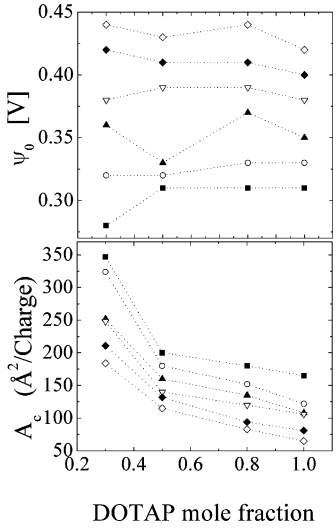

Figure 5. The parameters entering in eq 5 as a function of the salt concentration in the subphase, for DOTAP/DOPE (0.25/0.75), (0.50/0.50), (0.80/0.20), and (1/0) mixed monolayers: (upper panel) the potential ψ_0 and (lower panel) the area per charge A_c at different area per molecule: (■) 100 Å^2; (○) 90 Å^2; (▲) 80 Å^2; (▽) 70 Å^2; (◆) 60 Å^2; (◇) 55 Å^2.

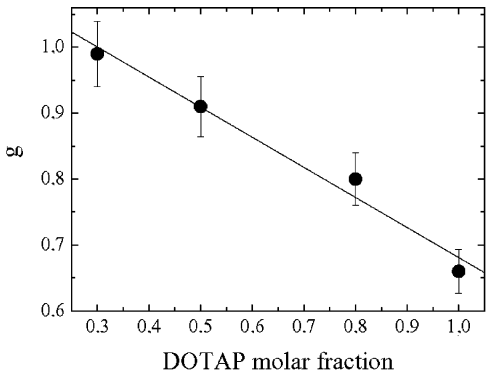

Figure 6. The charge renormalization parameter g for DOTAP−DOPE mixed monolayers calculated on the basis of relationship $(A/X)g = A_c$. The full line is the linear fit of the data.

and thus, the normal dipole moment component μ_N increases, as evidenced in Figure 5.

As expected, the values of A_c increase with the increase of the average area A per molecule.

The knowledge of the parameter A_c for different DOTAP/DOPE compositions of the mixed monolayer enables us to evaluate the factor g which defines the charge renormalization at the aqueous monolayer interface.

For each surface pressure of the monolayer, the effective area per charge A_c is related to the measured averaged molecular area A through the relation $(A/X)g = A_c$, where X is the fractional molar concentration of DOTAP. Figure 6 shows the dependence of g on the monolayer composition at a selected surface pressure of 35 nN/m. As can be expected, g decreases as the DOTAP molar fraction increases and reaches a value of about $g = 0.7$ in a pure DOTAP monolayer.

The value of g, for each surface pressure of the monolayer we have considered, indicates that a charge renormalization at the charged lipid−aqueous solution interface occurs

$$Q_{eff} = gQ_{bare} = 4\pi R_0^2 g\frac{X}{A_{CL}X + A_{NL}} \qquad (6)$$

where A_{CL} and A_{NL} are the areas per headgroup of the cationic

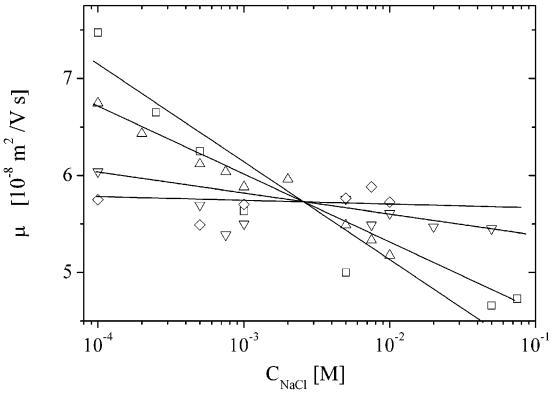

Figure 7. The electrophoretic mobility u as a function of the NaCl salt concentration in the bulk solution for mixed DOTAP/DOPE liposomes at different DOTAP/DOPE molar ratios: (□) pure DOTAP; (△) 0.65/0.35 DOTAP/DOPE; (▽) 0.50/0.50 DOTAP/DOPE; (○) 0.35/0.65 DOTAP/DOPE.

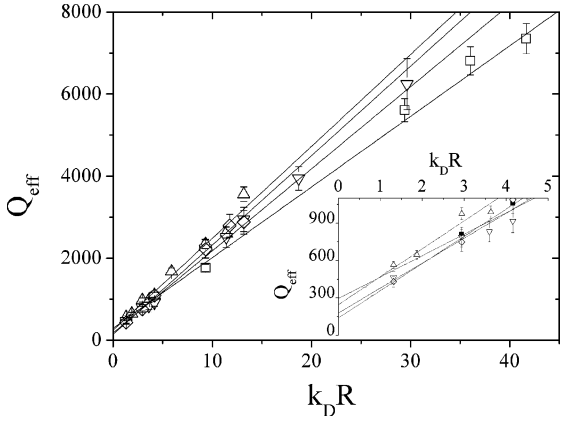

Figure 8. The effective Q_{eff} charge of DOTAP/DOPE mixed liposomes as a function of k_DR deduced from the measured ζ-potential on the basis of eq 7. The different values refer to different lipid mixtures: (□) DOTAP; (△) 0.65; (▽) 0.5; (◇) 0.35. The full curves are linear fits of the data. The inset shows the Q_{eff} dependence in the region of small k_DR values.

and neutral lipids and $X = C_{CL}/C_{NL}$ the cationic to neutral lipid ratio. The charge reduction is dependent on the surface charge of the monolayer and on its surface arrangement. However, this effect is relatively small; the maximum charge reduction is about 0.65 at the highest charge density at the surface pressure of 35 mN/m and progressively decreases with decreasing pressure (data not shown).

3.2. Spherical Interfaces. Spherical charged interfaces have been realized by means of spheroidal vesicles built up by cationic lipids dispersed in an aqueous solution. The surface charge density has been varied by using, as above in the case of a planar surface, a mixture of cationic and neutral lipids whose relative concentration was varied from 1 (which corresponds to a fully charged surface) to 0.35 (which corresponds to a partially charged surface). The two lipids employed were DOTAP and DOPE, whose miscibility was previously ascertained through thermodynamic measurements. The vesicle mean diameter was determined from standard dynamic light scattering technique, and values ranging from 80 to 100 nm were observed for mixed DOTAP/DOPE liposomes at the different compositions investigated.

In this case, the charge renormalization was estimated, following, at least in principle, the same procedure we employed in the planar interface analysis, where the surface potential ΔV was substituted by the ζ-potential and the comparison with the previous case was carried out by assuming for the spherical lipid bilayer a surface pressure of about 35 mN/m.[28] This value corresponds to the packing of a biological membrane and can be considered, almost as a first approximation, as the packing surface pressure at which lipid molecules self-assemble.

Moreover, also in this case, to make the comparison more appropriate, the ionic strength of the aqueous phase was varied by adding a simple 1:1 valent salt (NaCl), in the range from 5 mmol/L to 0.1 mol/L.

The evaluation of the effective charge at the vesicle surface in the presence of aqueous solutions of different ionic strengths proceeds through the measurement the electrophoretic mobility of the lipid vesicles under the influence of an external electric field. This technique is based on the principles of laser Doppler electrophoresis,[30] consisting of the analysis of the mixing of light scattered from a vesicle suspension and a reference beam of well-known frequency.

The electrophoretic mobility u of mixed DOTAP/DOPE liposomes in different salt content aqueous solutions are shown in Figure 7. In the case of vesicles with higher charge densities (DOTAP 0.75 and 0.65 mole fraction), u decreases with the salt concentration following the scaling law $u \sim c^{-0.5}$. This behavior is expected from the Smoluchowski limiting law $u \sim k_D^{-1} \sim c^{-0.5}$ for large k_DR, where k_D is the inverse of the Debye length.

At lower surface charge densities (DOTAP 0.35 and 0.5 mole fraction), the slope of the linear dependence on the salt concentration is larger and tends to values close to zero.

The mobility u was converted into a ζ-potential using the Smoluchowski relation $\zeta = Cu\eta/\epsilon_m$, where η and ϵ_m are the viscosity and the permittivity of the solvent, respectively, and C is a constant that depends on k_DR, the product of the radius R of the liposome and the inverse Debye screening length k_D. The limiting values of this constant are $C = 1$ for $(k_DR) \rightarrow \infty$ and $C = 1.5$ for $(k_DR) \rightarrow 0$.[8]

Finally, from the ζ-potential, by using the O'Brien−White equation, the effective "electrokinetic" charge as a function of the salt concentration can be determined

$$Q_{eff} = \frac{\epsilon_m K_B T k_D R^2}{e^2}\left[2\sinh\left(\frac{e\zeta}{2K_BT}\right) + \frac{4}{k_DR}\tanh\left(\frac{e\zeta}{4K_BT}\right)\right] \quad (7)$$

The results are reported in Figure 8, where the dependence of the effective (or electrokinetic) charge Q_{eff} of the lipid vesicle on the salt content is shown.

The extrapolation of this effective charge to zero salt content results in the charge that effectively must be associated to the vesicle in the electrostatic interactions, whose value varies from about 150 to 300 elementary charge as the surface charge is progressively increased, from DOTAP/DOPE 0.35 molar fraction to pure DOTAP liposomes (Figure 9). Although the accuracy of this quantity is moderate because the uncertainty in the linear fit of the data shown in Figure 9 was large, its value is very small when compared with the stoichiometric values calculated on the basis of a full dissociation of the ionic groups, resulting in an elementary positive charge per charged lipid molecule. In the case of pure DOTAP vesicles, 50 nm in radius, assuming a surface area per charge of about 60 Å^2, each vesicle should bear a charge of about $Q_{bare} \simeq 3.6 \times 10^4$ e. This charge progressively reduces to lower values as the concentration of DOPE is progressively increased (about $Q_{bare} \simeq 1.3 \times 10^4$ e for DOTAP/DOPE 0.35/0.65 molar fraction). Conversely to what happens in the case of planar surfaces (the renormalization factor varies between 1 and 0.7 for the different lipid compositions investigated), in this case, as can be seen in Figure

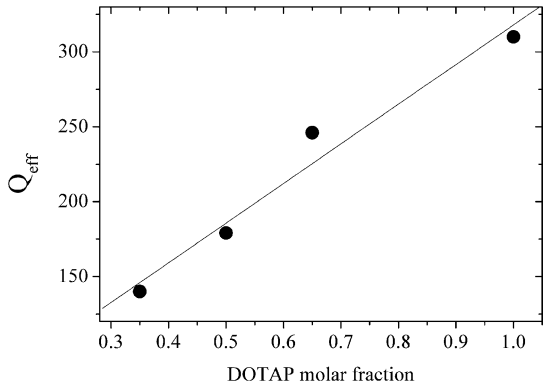

Figure 9. The values of the effective charge Q_{eff} extrapolated at $k_DR \rightarrow 0$, for mixed DOTAP/DOPE liposome of different compositions.

9, a very strong charge renormalization occurs. An effective charge of 200−300 protons/vesicle has been previously found, both experimentally[11,14] and theoretically.[13] For example, as pointed out by Haro-Perez et al.,[14] the structure factor of latex particles 80 nm in size determined from static light scattering experiments has been analyzed using as adjustable parameter an effective charge of $Q_{eff} = 330$ e, considerably smaller than the surface charge estimated by acid−base titration (in this case, $Q \simeq 2200$ e).

The relationship between the effective charge Q_{eff} and the bare charge of spherical colloidal particles has been recently analyzed by Aubouy et al.[13] who proposed an analytical approximation based on the nonlinear Poisson−Boltzmann equation. They obtained the following relationship

$$Q_{eff}\frac{l_B}{R} = 4k_DRT(x) + 2\left[5 - \frac{T(x)^4 + 3}{T(x)^2 + 1}\right]T(x) \qquad (8)$$

where the function $T(x)$ is defined as

$$T(x) = \frac{1}{x}(\sqrt{1 + x^2} - 1) \qquad (9)$$

with x defined as

$$x = \frac{Z_{bare}l_B}{R(2k_DR + 2)} \qquad (10)$$

where $Q_{bare} = Z_{bare}e$ is the bare charge of the particle. Although eq 8 is valid in the limit of large k_DR, it is accurate enough when $k_DR \geq 1$.

Figure 10 shows the comparison between the effective charge Q_{eff} and the values derived on the basis of eq 8 as a function of k_DR, considering the stoichiometric charge of the liposome particle (renormalized by the parameter g, gQ_{bare}). As can be seen, a very satisfactory agreement is found.

4. Conclusions

The charge renormalization in the limit of low salt content in mesoscopic heterogeneous systems with planar or spherical lipidic interfaces results in a reduction of the electric charge that actually is involved in the electrostatic interactions. This renormalization depends either on the bare charge or on the geometry of the interface.

In the case of planar monolayers and spherical bilayers, we have compared the effective surface charge derived from the measurements of the surface potential (in monolayers, at a pressure of 35 mN/m) or from the measurements of the

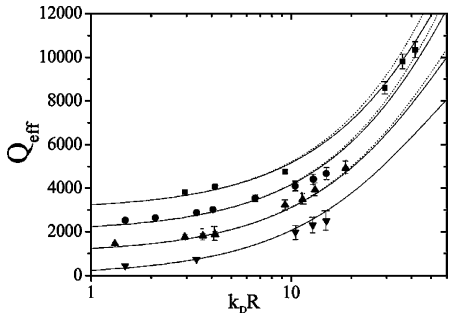

Figure 10. The effective charge Q_{eff} of the mixed DOTAP/DOPE liposome particles as a function of k_DR compared with the values calculated on the basis of eq 7. The bare charge of the particle is assumed to be $Z_{bare} = 3 \times 10^4$ for pure DOTAP liposome, and this value is progressively reduced in mixed DOTAP/DOPE liposome according to the bilayer composition, gZ_{bare}. The full lines are calculated by taking into account the renormalization factor g and considering the bare charge as gQ_{bare}. The dotted lines are calculated with the approximation $g = 1$. The data are shifted along the ordinate axis by an appropriate quantity, for clarity of presentation.

ζ-potential (in spherical vesicles) to the "bare" charge expected on the basis of the stoichiometry of the lipid mixture.

These data support evidence that the effective charge depends on the geometry of the mesoscopic colloidal object and on the concentration of the disperding electrolyte solution.

However, while in the case of planar surfaces the presence of an adsorbed counterion layer must be postulated in order to reconcile the experiments with an interpretation based on Gouy−Chapman theory, in the case of spherical liposomes, the approach based on nonlinearized Poisson−Boltzmann theory appears adequate to describe the observed strongly nonlinear screening. Although the difference could be ascribed to an influence of the different geometry, this fact raises some doubts regarding the effectiveness of the use of an approach based on Gouy−Chapman theory to evaluate the amount of ionization at the interface, even more when the Gouy−Chapman model is employed for systems in a spherical geometry (such as liposomes).[22,31]

References and Notes

(1) Sanchez, C.; Soler-Illia, G. J. D. A. A.; Ribot, F.; Grosso, D. *C. R. Chim.* **2003**, *6*, 1131−1151.
(2) Felnerova, D.; Viret, J.-F.; Glück, R.; Moser, C. *Curr. Opin. Biotechnol.* **2004**, *15*, 518529.
(3) Andresen, T. L.; Jensen, S. S.; Jørgensen, K. *Prog. Lipid Res.* **2005**, *44*, 6897.
(4) Groenewold, J.; Kegel, W. K. *J. Phys. Chem. B* **2001**, *105*, 11702−11709.
(5) Stradner, A.; Sedgwick, H.; Cardinaux, F.; Poon, W. C. K.; Egelhaaf, S. U.; Schurtenberger, P. *Nature (London)* **2004**, *432*, 492495.
(6) Mossa, S.; Sciortino, F.; Zaccarelli, E.; Tartaglia, P. *Langmuir* **2004**, *20*, 10756−10763.
(7) Sciortino, F.; Tartaglia, P.; Zaccarelli, E. arXiv:cond-mat/0505453.
(8) Quesada-Prez, M.; Callejas-Fernández, J.; Hidalgo-Alvarez, A. R. *Adv. Colloid Interface Sci.* **2002**, *95*, 295−315.
(9) Russel, W. B.; Saville, D. A.; Schowalter, W. R. *Colloidal Dispersions*; Cambridge University Press: Cambridge, MA, 1992.
(10) Alexander, S.; Chaikin, P. M.; Grant, P.; Morales, G. J.; Pincus, P.; Hone, D. *J. Chem. Phys.* **1984**, *80*, 5776−5781.
(11) Crocker, J. C.; Grier, D. G. *Phys. Rev. Lett.* **1994**, *73*, 352−355.
(12) Wette, P.; Schöpe, H. J.; Palberg, T. *J. Chem. Phys.* **2002**, *116*, 10981−10988.
(13) Aubouy, M.; Trizac, E.; Bocquet, L. *J. Phys. A: Math. Gen.* **2003**, *36*, 5835−5840.
(14) Haro-Pérez, C.; Quesada-Pérez, M.; Callejas-Fernández, J.; Casals, E.; Estelrich, J.; Hidalgo-Álvarez, R. *J. Chem. Phys.* **2003**, *118*, 5167−5173.
(15) Oosawa, F. *Polyelectrolytes*; Marcel Dekker: New York, 1971.
(16) Manning, G. S. *J. Chem. Phys.* **1969**, *51*, 924−933.
(17) Manning, G. S. *Q. Rev. Biophys.* **1978**, *11*, 179−246.

(18) Belloni, L. Interactions electrostatiques dans les solutions aqueuses de polyelectrolytes. Thesis, University of Paris VI, France, 1982.
(19) Belloni, L. *Chem. Phys.* **1985**, *99*, 43−54.
(20) Crocker, J. C.; Grier, D. G. *Phys. Rev. Lett.* **1996**, *77*, 1897−1900.
(21) Cevc, G. *Biochim. Biophys. Acta* **1990**, *1031*, 311−382.
(22) Zuidam, N. J.; Barenholz, Y. *Biochim. Biophys. Acta* **1997**, *1329*, 211−222.
(23) Hirsch-Lerner, D.; Zhang, M.; Eliyahu, H.; Ferrari, M. E.; Wheeler, C. J.; Barenholz, Y. *Biochim. Biophys. Acta* **2005**, *1714*, 71−84.
(24) Jones, M. N.; Chapman, D. *Micelles, Monolayers, and Biomembranes*; John Wiley and Sons: Chichester, UK, 1994.
(25) Yamins, H. G.; Zisman, W. A. *J. Chem. Phys.* **1933**, *1*, 656−661.
(26) Peterson, I. R. *Rev. Sci. Instrum.* **1999**, *70*, 3418−3424.
(27) Taylor, D. M. *Adv. Colloid Interface Sci.* **2000**, *87*, 183−203.
(28) Dynarowicz-Łątka, P.; Dhanabalan, A.; Oliveira, O. N. *J. Adv. Colloid Interface Sci.* **2001**, *91*, 221−293.
(29) Hunter, R. J. *Zeta potential in colloid science. Principles and applications*; Academic Press: London, 1981.
(30) McNeil-Watson, F.; Tscharnuter, W.; Miller, J. *Colloids Surf., A* **1998**, *140*, 53−57.
(31) Banerjee, R.; Das, P. K.; Chaudhuri, A. *Biochim. Biophys. Acta* **1998**, *1373*, 299−308.